

AD-A085722

AD

TECHNICAL REPORT ARBRL-TR-02239

THE DETAILED MODELING OF PREMIXED,
LAMINAR STEADY-STATE FLAMES TO OBTAIN
VALIDATED REACTION NETWORKS. I. OZONE.

J. M. Heimerl
T. P. Coffee

TECHNICAL
LIBRARY

April 1980



US ARMY ARMAMENT RESEARCH AND DEVELOPMENT COMMAND
BALLISTIC RESEARCH LABORATORY
ABERDEEN PROVING GROUND, MARYLAND

Approved for public release; distribution unlimited.

Destroy this report when it is no longer needed.
Do not return it to the originator.

Secondary distribution of this report by originating
or sponsoring activity is prohibited.

Additional copies of this report may be obtained
from the National Technical Information Service,
U.S. Department of Commerce, Springfield, Virginia
22151.

The findings in this report are not to be construed as
an official Department of the Army position, unless
so designated by other authorized documents.

*The use of trade names or manufacturers' names in this report
does not constitute endorsement of any commercial product.*

REPORT DOCUMENTATION PAGE		READ INSTRUCTIONS BEFORE COMPLETING FORM
1. REPORT NUMBER TECHNICAL REPORT ARBRL-TR- 02239	2. GOVT ACCESSION NO.	3. RECIPIENT'S CATALOG NUMBER
4. TITLE (and Subtitle) THE DETAILED MODELING OF PREMIXED, LAMINAR STEADY-STATE FLAMES TO OBTAIN VALIDATED REACTION NETWORKS. I. OZONE.		5. TYPE OF REPORT & PERIOD COVERED BRL TECHNICAL REPORT
7. AUTHOR(s) J. M. Heimerl T. P. Coffee		6. PERFORMING ORG. REPORT NUMBER
9. PERFORMING ORGANIZATION NAME AND ADDRESS US Army Armament Research and Development Command US Ballistic Research Laboratory ATTN: DRDAR-BLP Aberdeen Proving Ground, MD 21005		10. PROGRAM ELEMENT, PROJECT, TASK AREA & WORK UNIT NUMBERS 1L161102AH43
11. CONTROLLING OFFICE NAME AND ADDRESS US Army Amament Research and Development Command US Ballistic Research Laboratory ATTN: DRDAR-BL Aberdeen Proving Ground, MD 21005		12. REPORT DATE April 1980
14. MONITORING AGENCY NAME & ADDRESS (if different from Controlling Office)		13. NUMBER OF PAGES 52
		15. SECURITY CLASS. (of this report) UNCLASSIFIED
		15a. DECLASSIFICATION/DOWNGRADING SCHEDULE
16. DISTRIBUTION STATEMENT (of this Report)		
Approved for public release; distribution unlimited		
17. DISTRIBUTION STATEMENT (of the abstract entered in Block 20, if different from Report)		
18. SUPPLEMENTARY NOTES		
19. KEY WORDS (Continue on reverse side if necessary and identify by block number) Premixed laminar flame Elementary chemical reactions <i>flame propagation</i> Ozone flame Flame speeds Flame modeling Species profiles Species dependent transport Temperature profiles		
20. ABSTRACT (Continue on reverse side if necessary and identify by block number) (clt) We have employed species dependent input coefficients for the test case ozone in a one-dimensional model of a premixed, laminar, steady-state flame. Convenient expressions for the input coefficients are developed. These coefficients are based on independent measurements, i.e., no arbitrary parameters are used in the model. The governing equations are solved using a relaxation technique and the partial differential equation package, PDECOL, developed by Madsen and Sincovec. Species and temperature profiles and the burning velocities		

(Continued)

20. ABSTRACT (Continued)

are found over the range of initial ozone mole fraction of 0.25 to 1.00. The computed burning velocities are no more than 30% greater than the measurements of Streng and Grosse. Comparison with the computed results of Warnatz shows agreement within \pm 12%, even though he used quite different expressions for some of the kinetic coefficients. These differences are manifest in the atomic oxygen and temperature profiles at an initial ozone mole fraction of unity. A comparison of the model profiles indicates a need for measurements or *ab initio* calculations for the rate coefficient for the reaction $O_3 + O \rightarrow 2 O_2$ at temperatures in the range 1500-2000K.

UNCLASSIFIED

TABLE OF CONTENTS

	Page
LIST OF ILLUSTRATIONS	5
LIST OF TABLES	7
I. INTRODUCTION	9
II. THE FLAME EQUATIONS	11
III. PDECOL - A GENERAL PDE SOLVER	14
IV. INPUT COEFFICIENTS	15
A. Kinetic	15
B. Thermodynamic	16
C. Transport	18
V. RESULTS AND DISCUSSIONS	25
VI. SUMMARY	40
REFERENCES	41
GLOSSARY OF TERMS	45
DISTRIBUTION LIST	47

LIST OF ILLUSTRATIONS

Figure	Page
1. Temperature and Species Profiles for IOMF = 0.25, T_u = 300K and Total Pressure = 1 atmosphere	26
2. Temperature and Species Profiles for IOMF = 0.50, T_u = 300K and Total Pressure = 1 atmosphere	27
3. Temperature and Species Profiles for IOMF = 0.75, T_u = 300K and Total Pressure = 1 atmosphere	28
4. Temperature and Species Profiles for IOMF = 1.0, T_u = 300K and Total Pressure = 1 atmosphere	29
5. Burning Velocity vs. IOMF. Squares are the experimental points. Circles are computed from our model. The line is Streng and Grosse's expression for the burning velocity . .	30
6. Ratio of the Values of Warnatz' and Our Input Coefficients; e.g., the ratio $k_1, \text{Warnatz}/k_1, \text{this paper}$ is given by the curve identified by k_1	34
7. Our and Warnatz' Calculated Atomic Oxygen Profiles for IOMF = 1.0. (These curves are arbitrarily displaced for ease in viewing.) Dashed profile results from the substitution of Warnatz' expressions for k_1 and k_2 into our model	37
8. Our and Warnatz' Calculated Temperature Profiles for IOMF = 1.0. (These curves are arbitrarily displaced for ease in viewing.) Dashed profile results from the substitution of Warnatz' expressions for k_1 and k_2 into our model	38

LIST OF TABLES

Table	Page
1. KINETIC COEFFICIENTS	17
2. THERMODYNAMIC COEFFICIENTS	19
3. TRANSPORT COEFFICIENTS	20
4. LENNARD-JONES/STOCKMAYER PARAMETERS	23
5. COMPARISON OF OUR COMPUTED BURNING VELOCITIES WITH THE MEASUREMENTS OF STRENG AND GROSSE	31
6. PERCENTAGE CHANGE IN THE COMPUTED BURNING VELOCITY AT INITIAL OZONE MOLE FRACTIONS OF 0.25 AND 1.00 WHEN EACH INPUT COEFFICIENT IS MULTIPLIED BY A FACTOR OF 1.2	33
7. COMPARISON OF WARNATZ' COMPUTED BURNING VELOCITIES WITH OURS	33
8. SUCCESSIVE SUBSTITUTION OF WARNATZ' (W) KINETIC COEFFICIENTS FOR OURS (O) AT AN INITIAL OZONE FRACTION OF UNITY	36

I. INTRODUCTION

Advances in the development of laser based combustion diagnostic techniques, of numerical algorithms for solving ordinary and partial differential equations, and of larger capacity and higher speed computing machines have combined to enable one to begin to construct models of complex combustion phenomena that include fundamental physico-chemical processes. The necessary inputs to such models are data sets of (1) chemical reactions, including their rate coefficients, (2) thermodynamic coefficients and, (3) transport coefficients.

In the work presented here, we have used a one-dimensional, premixed, laminar, steady-state flame model to predict individual species and temperature profiles. The computed profiles are compared with experimental data to test the model. Essential agreement between measured and computed profiles is taken as validation of the model input parameters. On the other hand, discrepancies indicate those areas that are in need of further study.

We have studied the ozone flame as a test case because of its simplicity. There are three species: O, O₂, and O₃, related by the reactions



and



We emphasize that the requisite input data are obtained from independent experiments and that adjustable (arbitrary) parameters or average values

were not employed. Specifically, the thermodynamic, kinetic and laminar transport properties are both species and temperature dependent.

With few exceptions,¹⁻³ most other models of the ozone flame have emphasized mathematical approaches or numerical techniques.⁴⁻⁷ That is, their primary objective has been the development of methods of solution rather than detailed comparisons of model predictions and experimental results. Consequently these authors either employed mathematically non-essential assumptions that simplified the transport or employed kinetic coefficients that are incompatible with what is presently known, or both. They have also generally limited their illustrations to the single case of 0.25 initial ozone mole fraction (IOMF).

The object of this paper is to present as detailed an assembly of input parameters as practical, to describe the input coefficients by means of convenient expressions, to compare our model results with other results and to indicate future directions of investigation. We do this so that a complete verified set of realistic input parameters may become available for what has become a standard test case, the premixed laminar ozone flame.

¹F. Cramarossa and G. Dixon-Lewis, "Ozone Decomposition in Relation to the Problem of the Existence of Steady-State Flames", *Combustion and Flame* 16, 243-251 (1971).

²Kenneth A. Wilde, "Boundary-Value Solutions of the One-Dimensional Laminar Flame Propagation Equations", *Combustion and Flame* 18, 43-52, (1972).

³J. Warnatz, "Calculation of the Structure of Laminar Flat Flames I: Flame Velocity of Freely Propagating Ozone Decomposition Flames", *Ber. Bunsenges Phys. Chem.* 82, 193-200 (1978).

⁴Leon Bledjian, "Computation of Time-Dependent Laminar Flame Structure", *Combustion and Flame* 20, 5-17, (1973).

⁵Edwin S. Campbell, "A Theoretical Analysis of Chemical and Physical Processes in an Ozone Flame", *Chem. Engineering Sci.* 20, 311-329, (1965).

⁶Stephen B. Margolis, "Time-Dependent Solution of a Premixed Laminar Flame", *J. of Computational Phys.* 27, 410-427, (1978).

⁷J. O. Hirschfelder, C. F. Curtis and Dorothy E. Campbell, "The Theory of Flame Propagation. IV", *J. Phys. Chem.* 57, 403-414, (1953).

II. THE FLAME EQUATIONS

The derivation of the conservation equations for a multi-component reacting ideal gas mixture can be found in the literature.⁸⁻¹⁰ Here we are interested in those equations that adequately describe a one-dimensional, laminar, premixed flame that propagates in an unbounded medium. The effects of radiation, viscosity, thermal diffusion and body forces are ignored. Since the burning velocity is small compared with the local speed of sound, the pressure is taken to be constant.^{10,11}

The equations pertinent to our present case are:

Overall Continuity:

$$\frac{\partial \rho}{\partial t} + \frac{\partial (\rho u)}{\partial x} = 0 \quad (1)$$

Continuity of Species:

$$\rho \frac{\partial Y_k}{\partial t} + \rho u \frac{\partial Y_k}{\partial x} = - \frac{\partial}{\partial x} (\rho Y_k V_k) + R_k M_k, \quad k = 1, 2, \dots, N \quad (2)$$

and

Conservation of Energy:

$$\rho c_p \frac{\partial T}{\partial t} + \rho u c_p \frac{\partial T}{\partial x} = \frac{\partial}{\partial x} (\lambda \frac{\partial T}{\partial x}) - \sum_{k=1}^N R_k M_k h_k - \rho \sum_{k=1}^N c_p k Y_k V_k \frac{\partial T}{\partial x}, \quad (3)$$

where the variables are defined in the glossary. In equations (2) and (3), V_k is determined by the Stefan-Maxwell equations,

⁸J. O. Hirschfelder, C. F. Curtis and R. B. Bird, Molecular Theory of Gases and Liquids, 2nd Printing, Corrected, with notes, John Wiley and Sons, NY, (1964).

⁹R. B. Bird, W. S. Stewart and E. N. Lightfoot, Transport Phenomena, John Wiley and Sons, NY, (1960).

¹⁰F. A. Williams, Combustion Theory, Addison-Wesley, Reading, MA, (1965).

¹¹R. M. Fristrom and A. A. Westenberg, Flame Structure, McGraw-Hill, NY, (1965) p. 319.

$$\frac{\partial X_k}{\partial x} = \sum_{j=1}^N \frac{X_k X_j}{D_{kj}} (V_j - V_k). \quad (4)$$

The boundary conditions are the following ($t \geq 0$).

For $x = +\infty$

$$T = T_u \text{ and}$$

$$Y_k = Y_{ku}, \quad (k = 1, 2, \dots, N),$$

and for $x = -\infty$

$$\frac{\partial T}{\partial x} = \frac{\partial Y_k}{\partial x} = 0, \quad (k = 1, 2, \dots, N). \quad (5)$$

In order to avoid solving equation (1) a coordinate ψ is introduced such that

$$\psi(x, t) = \int_0^x \rho(x', t) dx'. \quad (6)$$

Then $\frac{\partial \psi}{\partial x} = \rho$ and $\frac{\partial \psi}{\partial t} = -\rho u + m_o(t)$, where $\rho u|_{x=0} = m_o(t)$.

With this notation equations (2) and (3) become

$$\frac{\partial Y_k}{\partial t} + m_o \frac{\partial Y_k}{\partial \psi} = -\frac{\partial}{\partial \psi} (\rho Y_k V_k) + R_k M_k / \rho \quad (7)$$

and

$$\frac{\partial T}{\partial t} + m_o \frac{\partial T}{\partial \psi} = \frac{1}{c_p} \frac{\partial}{\partial \psi} (\rho \lambda \frac{\partial T}{\partial \psi}) - \frac{1}{\rho c_p} \sum_{k=1}^N R_k M_k h_k - \sum_{k=1}^N \frac{c_p k}{c_p} \rho Y_k V_k \frac{\partial T}{\partial \psi} \quad (8)$$

respectively. The solution of equations (7) and (8) yields the steady state profiles of atomic oxygen, ozone and temperature. (In practice convenient dimensionless forms of equations (7) and (8) are solved.) The molecular oxygen profile is obtained from the relation

$$\sum_{k=1}^3 Y_k = 1.$$

The burning velocity, S_u , is defined as the velocity of the flame relative to the fluid at rest, i.e., at infinity. The value of S_u can be found from the steady state profiles by performing a coordinate transformation such that the flame appears stationary. In this new system all variables are independent of time; specifically,

$$\frac{\partial Y_k}{\partial t} = 0, \text{ and}$$

$$\frac{\partial \rho}{\partial t} = 0.$$

From equation (1) we then have

$$\partial(\rho u)/\partial x = 0, \text{ or } \rho u = \text{constant.}$$

Take any one of the equations (2) and integrate over any interval (a, b) to obtain

$$\rho u [Y_k(b) - Y_k(a)] = \int_a^b R_k M_k dx - \rho Y_k V_k \Big|_a^b . \quad (9)$$

Then

$$u(\infty) = \frac{\int_a^b R_k M_k dx - \rho Y_k V_k \Big|_a^b}{\rho(\infty)[Y_k(b) - Y_k(a)]} = \frac{\int_a^b \rho^{-1} R_k M_k d\psi - \rho Y_k V_k \Big|_a^b}{\rho(\infty)[Y_k(b) - Y_k(a)]} . \quad (10)$$

In this coordinate system $S_u = -u(\infty)$.

III. PDECOL - A GENERAL PDE SOLVER

The package PDECOL, developed by Madsen and Sincovec¹² was used to solve this problem. This is a general package for solving partial differential equations (PDE's) using the method of lines.

The spatial discretization is accomplished by finite element collocation methods based on B-splines.¹³ The basic assumption is that the solution can be written in the form

$$Y_k \approx \sum_{i=i}^{NC} C_k^{(i)}(t) B_i(\psi), \quad k=1\dots N, \quad \text{and}$$

$$T \approx \sum_{i=i}^{NC} C_{N+1}^{(i)}(t) B_i(\psi),$$

where the basis functions $B_i(\psi)$, $i=1 \dots NC$, are B-splines and span the solution space for any fixed t to within a small error tolerance. The time dependent coefficients $C_k^{(i)}$ are determined uniquely by requiring that the expansion above satisfy the given boundary conditions and that they satisfy equations (7) and (8) exactly at ($NC-2$) interior (collocation) points. If there is a null boundary condition, an extra collocation point is added. The B_i are piecewise polynomials of order KORD. Given a user supplied set of NB breakpoints (i.e., a set of strictly increasing locations where the polynomials are joined) and the number of continuity conditions, NCC, to be applied at the breakpoints, PDECOL generates a set $NC = KORD(NB-1) - NCC(NB-2)$ basis functions and collocation points. Since by definition a B-spline is zero except over a small interval, at any collocation point no more than KORD of the B-splines are nonzero. So the system of ODE's for the coefficients $C_k^{(i)}$ will not be fully coupled.

¹²B. K. Madsen and R. F. Sincovec, "PDECOL: General Collocation Software for Partial Differential Equations", Preprint UCRL-78263 (Rev 1) Lawrence Livermore Laboratory, (1977).

¹³C. de Boor, "Package for Calculating With B-Splines", Siam. J. Numer. Anal. 14, 441-472, (1977).

This system of ODE's is integrated in time, using a variant of the Gear integrator. The appropriate banded Jacobian is generated internally by the program. Once the integrator has reached a desired output time t , the values of Y_k and T can be obtained for any ψ by substituting into the expansion.

The definition of the set of breakpoints that determines the spatial discretization is crucial. They must be chosen close enough that spatial errors do not destroy the solution yet not so dense that one's computer resources are exceeded. There is at present no way of determining an optimum set of breakpoints for a given problem other than trial and error. We have developed¹⁴ a method of concentrating our breakpoints in the steep flame-front, where accuracy is necessary. This method is similar to a procedure developed by Spalding and Stephenson¹⁵ for use in a finite difference code.

With initial guessed profiles for the ozone flame and with values of KORD = 6, NCC = 5 and $59 < NB < 70$, the program coding has executed in 30 to 60 seconds on the BRL Cyber 76 and has required about 80,000 words of core. A listing of the program is given in reference 14.

IV. INPUT COEFFICIENTS

A. Kinetic

Reaction (1) is the *sine qua non* of the ozone flame and as such is the single most important reaction. Thus we require the expression of k_1 to be valid over the range of adiabatic flame temperatures, $\sim 1000K$ - $3000K$. Available reviews¹⁶⁻¹⁷ recommend expressions that are valid only

¹⁴T. P. Coffee and J. M. Heimerl, "A Method for Computing the Flame Speed for a Laminar, Premixed, One Dimensional Flame", BRL Technical Report, ARBRL-TR-02212, Jan 80. (AD#A082803)

¹⁵D. B. Spalding and P. L. Stephenson, "Laminar Flame Propagation in Hydrogen and Bromine Mixtures", Proc. Roy. Soc. London A324, 315-337, 1971. (See also), D. B. Spalding, P. L. Stephenson and R. G. Taylor, "A Calculation Procedure for the Prediction of Laminar Flame Speeds", Combustion and Flame, 17, 55-64, 1971.

¹⁶D. L. Baulch, D. D. Drysdale, J. Duxbury and S. J. Grant, Evaluated Kinetic Data for High Temperature Reactions, Vol 3, Homogeneous gas phase reactions of the O_2/O_3 system, the $CO/O_2/H_2$ system and of sulphur containing species. Butterworths, Boston, (1976).

¹⁷Harold S. Johnston, "Gas Phase Reaction Kinetics of Neutral Oxygen Species", NSRDS-NBS-20, September 1968.

up to 1000K. Recently we¹⁸ have critically examined the high temperature shock tube results of Michael¹⁹ (971K-1384K) and of Center and Kung²⁰ (2041K-2941K) and found the expression listed in Table 1. This expression describes all the direct experimental data available for k_1 and is valid over the range 300K-3000K. To a good approximation it is independent of any set of experimental data. (For a more detailed discussion, see reference 18).

The expression for k_2 and k_3 have been taken from the review literature of Hampson²¹ and Johnston,¹⁷ respectively. (Hampson's and Johnston's expression for k_2 yield values that differ by 15% or less over the range $600K \leq T \leq 3000K$). The expression of k_{-1} and k_{-2} have been derived from the forward rate coefficients and the corresponding equilibrium constants. The expression for k_{-3} is taken from Johnston. Over the range $1000K \leq T \leq 3000K$ the value of the equilibrium constants for reaction 3 as computed from Johnston's expressions for k_3 and k_{-3} is at most 20% greater than published equilibrium values.¹⁶

The rate coefficient may vary with the identity of the chaperon or third body, M. The chaperon relationships used are $k_1(M=O_2) = 0.44$ $k_1(M=O_3),^{17}$ $k_3(M=0) = 3.6$ $k_3(M=O_2),^{16}$ $k_1(M=0) = k_1(M=O_2)$ and $k_3(M=O_3) = k_3(M=O_2)$. Only the first relationship has been found to be important.

B. Thermodynamic

The enthalpy and heat capacity are functions of species and of temperature. The JANAF²² values for the allotropes of oxygen are described to better than a few parts per thousand over the temperature range 300K-

¹⁸ J. M. Heimerl and T. P. Coffee, "The Unimolecular Ozone Decomposition Reaction", *Combustion and Flame*, 35, 117-123, 1979. For a complete listing of all direct measurements, see BRL Technical Report ARBRL-TR-02185, Aug 79. (AD#A076966)

¹⁹ J. V. Michael, "Thermal Decomposition of Ozone", *J. Chem. Phys.* 54, 4455-4459, (1971).

²⁰ R. E. Center and R. T. V. Kung, "Shock Tube Study of the Thermal Decomposition of O_3 From 1000 to 3000°K", *J. Chem. Phys.* 62, 801-807, (1975).

²¹ R. F. Hampson, (ed), "Survey of Photochemical and Rate Data for Twenty-Eight Reactions of Interest in Atmospheric Chemistry", *J. Phys. Chem. Ref. Data* 2, 267-312, (1973).

²² D. R. Stull and H. Prophet, JANAF Thermochemical Tables, 2nd Edition, NSRDS-NBS-37, June 1971.

TABLE 1. KINETIC COEFFICIENTS

COEFFICIENT	EXPRESSION	REFERENCE	REMARKS
k_1	$4.31 \times 10^{14} \exp(-11,161/T) \text{ cm}^3 \text{ mole}^{-1} \text{ s}^{-1}$	18	$300\text{K} \leq T \leq 3000\text{K}, M=0_3$
k_{-1}	$1.2 \times 10^{13} \exp(+976/T) \text{ cm}^6 \text{ mole}^{-2} \text{ s}^{-1}$		Derived from equilibrium const.
k_2	$1.14 \times 10^{13} \exp(-2300/T) \text{ cm}^3 \text{ mole}^{-1} \text{ s}^{-1}$	21	$200\text{K} \leq T \leq 1000\text{K}$
k_{-2}	$1.19 \times 10^{13} \exp(-50600/T) \text{ cm}^3 \text{ mole}^{-1} \text{ s}^{-1}$		Derived from equilibrium const.
k_3	$1.38 \times 10^{18} T^{-1} \exp(-171/T) \text{ cm}^6 \text{ mole}^{-2} \text{ s}^{-1}$	17	$1000\text{K} \leq T \leq 8000\text{K}, M=0_2$
k_{-3}	$2.75 \times 10^{19} T^{-1} \exp(-59732/T) \text{ cm}^3 \text{ mole}^{-1} \text{ s}^{-1}$	17	$1000\text{K} \leq T \leq 8000\text{K}, M=0_2$

3000K by the polynomial fits of Gordon and McBride.²³ These fits take the form:

$$H_T^0 = R(a_0 + \sum_{n=1}^5 a_n T^n / n)$$

and

$$C_p = R \sum_{n=1}^5 a_n T^{n-1},$$

where the coefficients are listed in Table 2.

C. Transport

The transport coefficients used for the ozone flame are listed in Table 3. (The subscripts 1, 2, and 3 for the transport coefficients stand for O, O₂ and O₃ respectively). Expressions for λ₁, λ₂ and pD₁₂ have been taken from the literature. Dalgarno and Smith²⁴ have computed the thermal conductivity for atomic oxygen up to 100,000K and derive an analytic expression for λ₁ valid over the range 100K-2000K. Hanley and Ely²⁵ have critically reviewed the thermal conductivity data for molecular oxygen and have tabulated values for λ₂ over the range 80K-2000K. Using the functional form ATB we have obtained a fit to their tabular values over the range 300K-2000K which fit has an overall root-mean-square error of ~1% and a maximum error of ~2%. Marrero and Mason²⁶ have critically reviewed data for pD₁₂ and determined an expression valid over the temperature range 280K-10,000K. It has an estimated uncertainty of ± 25% for temperatures above 1000K.

²³S. Gordon and B. J. McBride, "Computer Program for Calculation of Complex Chemical Equilibrium Compositions, Rocket Performance, Incident and Reflected Shocks, and Chapman-Jouguet Detonations", NASA-SP-273, (1971), (1976 program version).

²⁴A. Dalgarno and F. J. Smith, "The Thermal Conductivity and Viscosity of Atomic Oxygen", *Planet Spac. Sci.* 9, 1-2, (1962).

²⁵H. J. M. Hanley and J. F. Ely, "The Viscosity and Thermal Conductivity Coefficients of Dilute Nitrogen and Oxygen", *J. Phys. Chem. Ref. Data*, 2, 735-755, (1973).

²⁶T. R. Marrero and E. A. Mason, "Gaseous Diffusion Coefficients", *J. Phys. Chem. Ref. Data* 1, 3-118, (1972).

TABLE 2. THERMODYNAMIC COEFFICIENTS

Species	Range	a ₁	a ₂	a ₃	a ₄	a ₅	a ₀
O ₀	U	0.25352638E+01	-0.14371898E-04	-0.11360139E-07	0.66005131E-11	-0.61181626E-15	0.29230265E+05
	L	0.29558662E+01	-0.17061536E-02	0.25925154E-05	-0.17837980E-08	0.45709012E-12	0.29143654E+05
O ₂	U	0.36219535E+01	0.73618264E-03	-0.19652228E-06	0.36201558E-10	-0.28945627E-14	-0.12019825E+04
	L	0.36255985E+01	-0.18782184E-02	0.70554544E-05	-0.67635137E-08	0.21555993E-11	-0.10475226E+04
O ₃	U	0.54665239E+01	0.17326031E-02	-0.72204889E-06	0.13721660E-09	-0.96233828E-14	0.15214096E+05
	L	0.24660617E+01	0.91703209E-02	-0.49698480E-05	-0.20634230E-08	0.20015595E-11	0.16059556E+05
19	U:	1000K	$\leq T \leq 6000K$				
	L:	300K	$\leq T \leq 1000K$				

TABLE 3. TRANSPORT COEFFICIENTS

Transport Coefficient	Expression	References
λ_1^a	$1.60 \times 10^{-6} T^{0.71}$	Dalgarno and Smith, 24
λ_2	$5.74 \times 10^{-7} T^{0.827}$	Hanley and Ely, 25
λ_3	$3.90 \times 10^{-7} T^{0.842}$	This work
pD_{12}^b	$1.32 \times 10^{-5} T^{1.774}$	Marrero and Mason, 26
pD_{13}	$1.66 \times 10^{-5} T^{1.665}$	This work
pD_{23}	$1.18 \times 10^{-5} T^{1.665}$	This work

^aHeat conductivity in units of cal-cm⁻¹-s⁻¹-K⁻¹.^bPressure multiplied by binary diffusion coefficient in units of atmos-cm²-s⁻¹.

To complete the set of input coefficients expressions for λ_3 , pD_{23} and pD_{13} must be found. To accomplish this we first obtain from viscosity data, Lennard-Jones (L-J) parameters for O and O₂ and Stockmayer parameters for O₃. Then theoretical formalisms^{8,27} are used to determine values for each transport coefficient as a function of temperature. Finally a fit of the form AT^B is made to the values and listed in Table 3. An outline of the details follows.

The L-J parameter ϵ_i/k is found from the ratio of the values of the viscosity at two temperatures.²⁸ The atomic oxygen viscosity is taken from the expression of Dalgarno and Smith,²⁴ i.e., $\eta_1 = 3.34 \times 10^{-6} T^{0.71} \text{ gm-cm}^{-1}\text{-s}^{-1}$, $100\text{K} < T < 2000\text{K}$. The molecular oxygen viscosity is taken from the tabular data of Hanley and Ely.²⁵ (We elect to determine our own set of L-J parameters for O₂ rather than use Svehla's²⁹ because Hanley and Ely noted internal inconsistencies in certain viscosity measurements that were available to Svehla). Having found ϵ_i/k we can determine the L-J parameter σ_i from a direct substitution into

$$\eta_i(T) = \frac{266.93 \times 10^{-7} (M_i T)^{1/2} f(T_i^*)}{\sigma_i^2 \Omega^{2,2} (T_i^*)} \text{ gm-cm}^{-1}\text{-s}^{-1} \quad (11)$$

In practice we fix 300K as the first temperature and compute sets of L-J parameters for each second temperature in the interval 400K-2000K in steps of 100K. The L-J parameters that give the best fit to the viscosity data in a least squares sense are chosen and listed in Table 4. Over the range 300K-2000K our L-J parameters for molecular oxygen reproduce the tabular viscosity of Hanley and Ely to within 2% while Svehla's L-J parameters ($\epsilon_2/k = 106.7\text{K}$ and $\sigma_2 = 3.467\text{\AA}$) reproduce the same data within 4%.

The determination of the Stockmayer parameters for ozone is complicated by the fact that we have available only the viscosity of ozone-molecular oxygen mixtures. Tretter³⁰ records five measurements of the mixture viscosity of nearly equal molar volumes of O₂ and O₃ at 194K,

²⁷ R. C. Reid and T. K. Sherwood, The Properties of Gases and Liquids, 2nd Edition, McGraw-Hill, NY, (1966).

²⁸ J. O. Hirschfelder, C. F. Curtis and R. B. Bird, op. cit., p. 562.

²⁹ R. A. Svehla, "Estimated Viscosities and Thermal Conductivities of Gases at High Temperatures", NASA Tech. Report R-132, Lewis Res. Ct., Cleveland, Ohio, (1962).

³⁰ V. J. Tretter, An Experimental Determination of the Viscosity of Gaseous Ozone, M. S. thesis, U. of Idaho, (1966), unpublished.

273K and 295K. The procedure we have used to recover the ozone Stockmayer parameters from Tretter's data is as follows.

The expressions for the mixture viscosity as given by³¹ are functions of the L-J (Stockmayer) parameters, the temperature, molar composition and certain combining rules. For the O₂/O₃ mixture the L-J parameters for molecular oxygen are determined above and the temperature and composition are fixed by the experimental conditions. The empirical polar/non-polar combining rules³² are

$$\sigma_{23} = 0.5 (\sigma_2 + \sigma_3) \xi^{-1/6} \quad (12)$$

and

$$\epsilon_{23} = (\epsilon_2 \epsilon_3)^{1/2} \xi^2,$$

where $\xi = 1 + 0.25 \alpha_2 \mu_3^2 [\sigma_2^3 \sigma_3^3 (\epsilon_2 \epsilon_3)^{1/2}]^{-1}$. (The value used for the mean dipole polarizability of molecular oxygen, α_2 , is 1.6×10^{-24} cm³.^{27,33} The ozone dipole moment is taken as the average of the four values listed by McCellan;³⁴ i.e., $\mu_3 = 0.57 \times 10^{-18}$ dyne 1/2-cm².) The only unknowns in the mixture viscosity expressions are the Stockmayer parameters for ozone. A search is made over the two dimensional space of the Stockmayer parameters, pairs of parameters are selected and a mixture viscosity computed. A computed value is compared with the corresponding measured value and a root-mean-square (RMS) error is determined for the five temperature/composition conditions of the measurements. The minimum RMS error then determines the ozone Stockmayer parameters listed in Table 4. This procedure with Svehla's L-J parameters for molecular oxygen results in no essential change in the Stockmayer parameters for ozone.

The Stockmayer parameters for ozone are used in the appropriate form of equation (11) to find the ozone viscosity as a function of temperature. We find $\eta_3(T) = 4.24 \times 10^{-6} T^{0.65}$ gm-cm⁻¹-s⁻¹. Finally λ_3 is

³¹J. O. Hirschfelder, C. F. Curtis and R. B. Bird, op. cit., p. 530.

³²J. O. Hirschfelder, C. F. Curtis and R. B. Bird, op. cit., p. 600.

³³J. O. Hirschfelder, C. F. Curtis and R. B. Bird, op. cit., p. 950.

³⁴A. L. McCellan, Tables of Experimental Dipole Moments, W. H. Freeman and Co., San Francisco, (1963).

TABLE 4. LENNARD-JONES/STOCKMAYER PARAMETERS

Species	σ (Å)	ϵ/k (K)
O	2.947	127.2
O ₂	3.372	128.7
O ₃	4.69	39.4

found from η_3 by means of Reid and Sherwood's²⁷ recommended relationship between heat conductivity and viscosity, the Bromley analysis.

Using the parameters listed in Table 4 and the empirical combining laws given by equation (12) the diffusion coefficients pD_{13} and pD_{23} are computed as functions of temperature from the expression^{8,27}

$$pD_{ij} = \frac{2.628 \times 10^{-3} [T^3 (M_i + M_j) / 2 M_i M_j]^{1/2}}{\sigma_{ij}^2 \Omega^{1,1} (T_{ij}^*)} \text{ atmos-cm}^2 \text{-s}^{-1}. \quad (13)$$

Measurements for comparison are all but non-existent. Hildebrand³⁵ has discovered an empirical correlation that links the heat capacity of a gas with its viscosity at 298K. Using the ozone heat capacity of 9.4 cal-mole-1-K-1 at 298K²² and Hildebrand's correlation, we find $\eta_3(298K) = 164 \times 10^{-6}$ gm-cm-1-s-1. The value computed from our expression for η_3 (298K) is 168×10^{-6} gm-cm-1-s-1. Yastrebov³⁶ has estimated λ_3 at room temperature to be about three-quarters that of λ_2 . From Table 3 we find $0.75 \lambda_2$ (300K) = 4.82×10^{-5} cal-cm-1-s-1-K-1 and λ_3 (300K) = 4.75×10^{-5} cal-cm-1-s-1-K-1. Houzelot and Villermaux are reported³⁷ to have measured $D_{23} = 0.15 \text{ cm}^2 \text{-s}^{-1}$ at one atmosphere and 25°C. From Table 3 we find $D_{23}(298K) = 0.155 \text{ cm}^2 \text{-s}^{-1}$.

Another independent check can be made. From the L-J parameters for O and O₂, $(pD_{12})_{LJ}$ can be formed using the appropriate analogue of equation (13) and equation (12) ($\mu_1 = \mu_2 = 0$ implies $\xi = 1$). This computation yields the fit $(pD_{12})_{LJ} = 2.01 \times 10^{-5} T^{1.687}$ atmos-cm²-s⁻¹ over the range 300K - 2000K. The ratio $(pD_{12})_{LJ}$ to pD_{12} shows a monotonic decrease from 0.92 at 300K to 0.78 at 2000K. This comparison provides us with a measure of the efficacy of the procedures outlined above.

³⁵ J. H. Hildebrand, *Mole. Phys.*, 35, 519-523, (1978).

³⁶ V. V. Yastrebov, "The Physical Chemistry of Concentrated Ozone, VIII. Thermal Propagation of Flame in Gaseous Ozone Mixtures", *Russian J. of Phys. Chem.*, 34, 21-23, (1960).

³⁷ J. L. Houzelot and J. Villermaux, "Measurement of the Molecular Diffusivity of Ozone Oxygen", *C. R. Acad. Sci. Ser. C* 1971, 273, 258-60. As quoted by *Chem. Abstracts* 74, 252, (1971).

Equation (3) requires an expression for the heat conductivity of the mixture, λ . We have used³⁸

$$\lambda = 0.5 \sum_{i=1}^N X_i \lambda_i + \left(\sum_{i=1}^N X_i / \lambda_i \right)^{-1}$$

V. RESULTS AND DISCUSSION

Figures 1-4 show our computed profiles for four initial ozone mole fractions (IOMF's). For each IOMF $T_u = 300K$ and the total pressure is one atmosphere. We do not know of any experimental profiles for comparison and so by our definition (see Introduction) the validation of the ozone flame remains to be done. However, experimental burning velocities are available.

Figure 5 shows the burning velocity as a function of IOMF. Our computed values of the velocities are plotted as circles and the experimental data of Streng and Grosse³⁹ are shown as squares. The solid line is their expression for the burning velocity and is given by

$$S_u = 563 X_{O_3} - 88.8 \text{ cm/s.} \quad (14)$$

Table 5 lists our computed and the experimental values for the burning velocity. This right-hand column shows that between IOMF of 0.25 and 1.00, our computed values are 5 to 28% greater than the experimental values. Though no exact figures are given, Streng and Grosse state that for measurements less than 0.3 IOMF their experimental results are less accurate. Thus the 38% discrepancy for 0.20 IOMF is not necessarily a defect of the model.

Tests were made¹⁴ at IOMF = 0.25 and 1.0 to examine the sensitivity of the computed burning velocity to changes in the number of breakpoints, in the polynomial order of the spline functions, KORD, and in the number of continuity conditions imposed at the breakpoints, NCC. For each case we started the model from a standard profile and ended the exercise at a time sufficient to ensure that steady state had been achieved. For our standard conditions KORD = 6 and NCC = 5 a doubling of the number of

³⁸Y. S. Touloukian, P. E. Liley and S. C. Saxena, Thermophysical Properties of Matter, Vol. 3, Thermal Conductivity, Nonmetallic Liquids and Gases, IFI/Plenum, NY-Washington, (1970), p 45a.

³⁹A. G. Streng and A. V. Grosse, "The Ozone to Oxygen Flame", Sixth Symposium (International) on Combustion, Reinhold Publishing Company, (1957), pp 264-273.

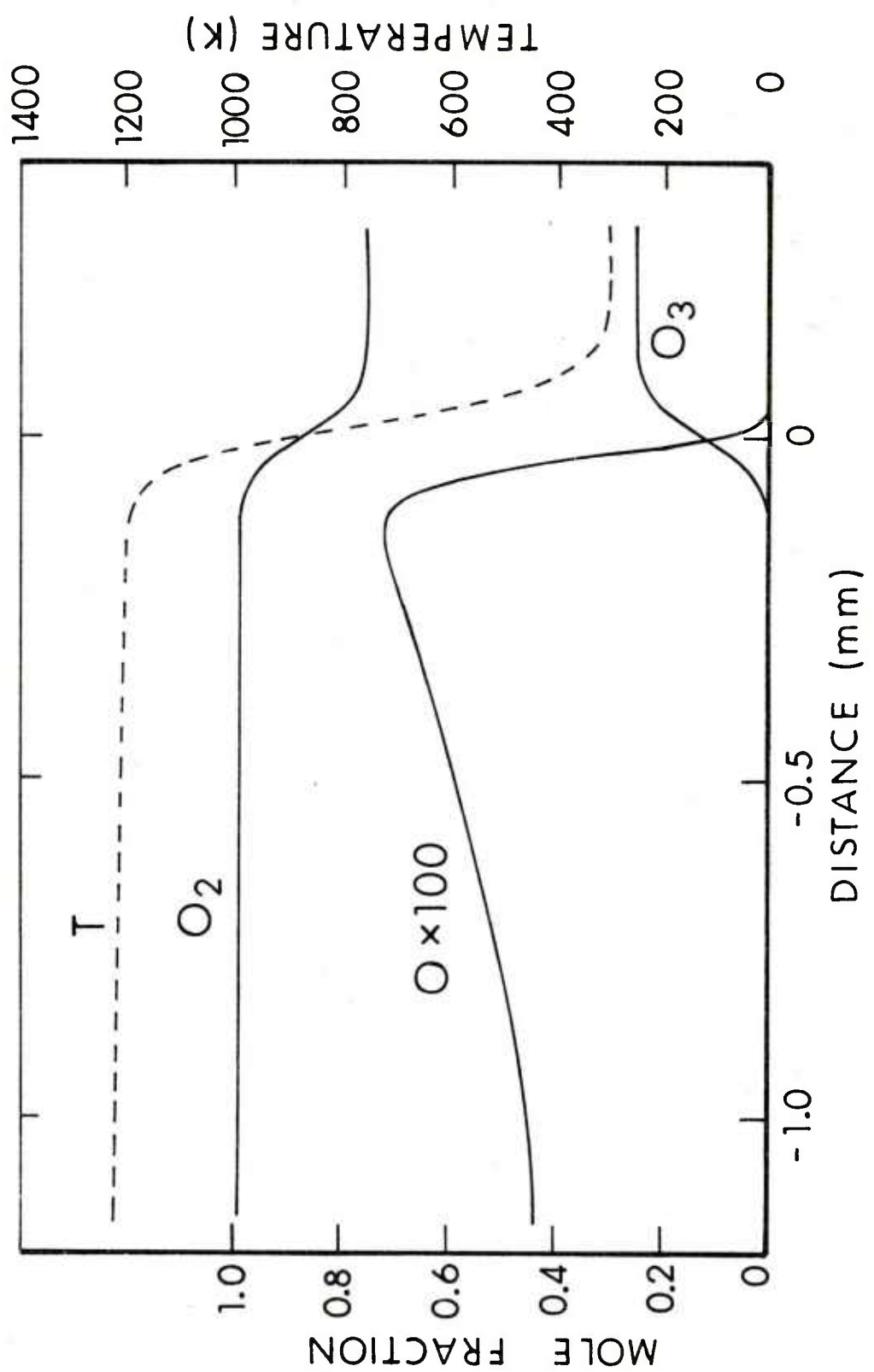


Figure 1. Temperature and Species Profiles for $10MF = 0.25$, $T_u = 300K$ and Total Pressure = 1 atmosphere.

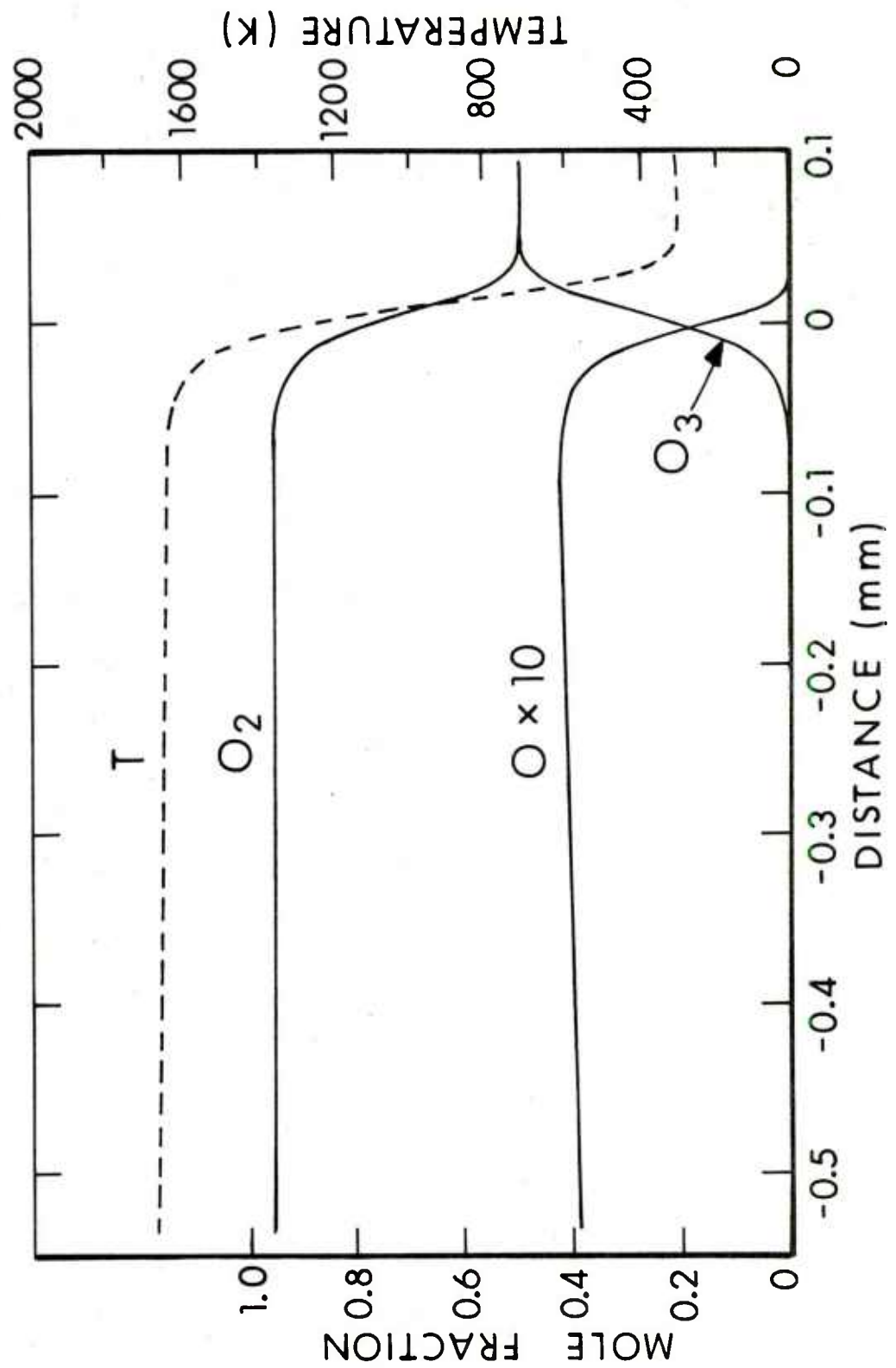


Figure 2. Temperature and Species Profiles for $10MF = 0.50$, $T_u = 300K$ and Total Pressure = 1 atmosphere.

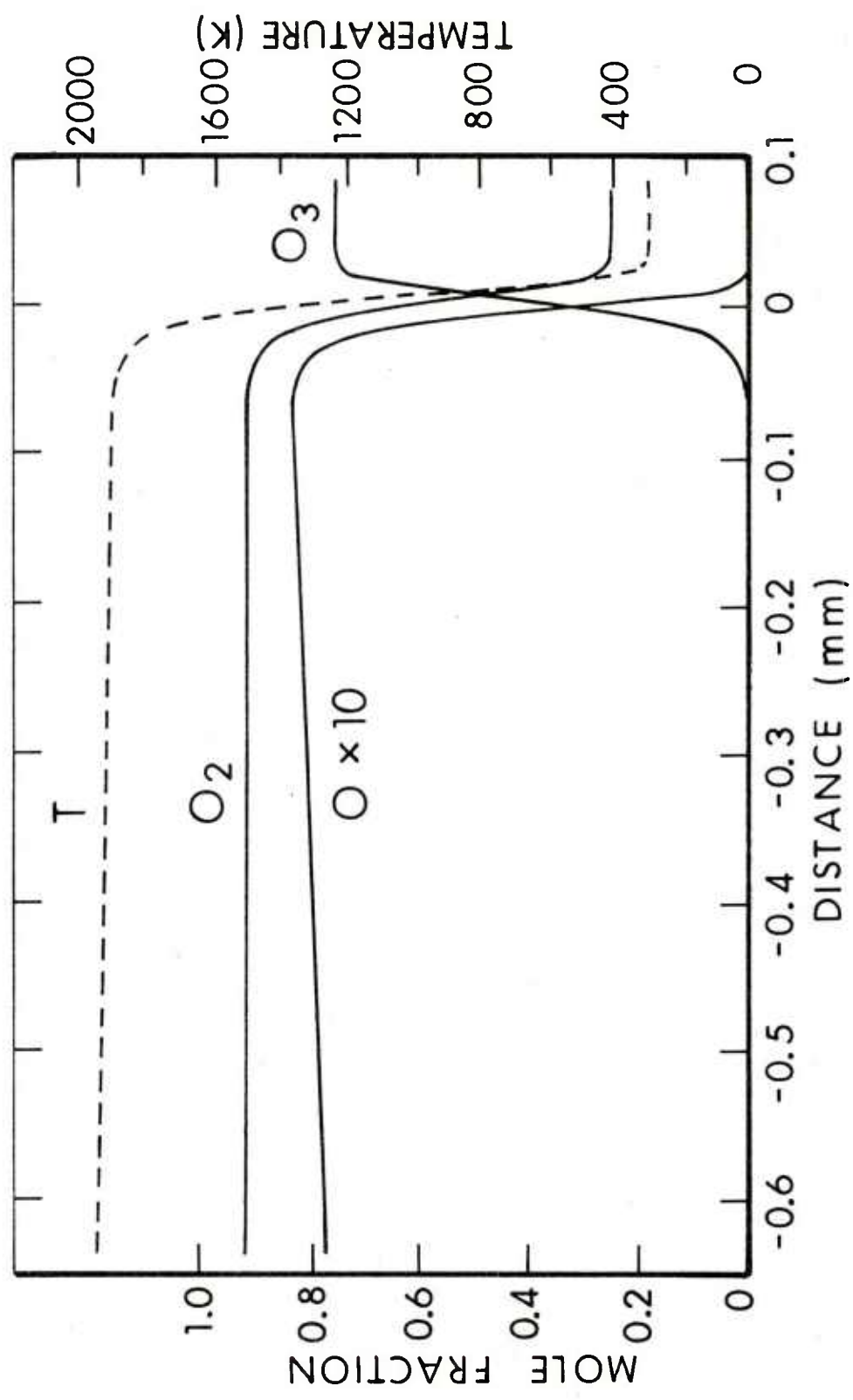


Figure 3. Temperature and Species Profiles for $I_{OMF} = 0.75$, $T_u = 300K$ and Total Pressure = 1 atmosphere.

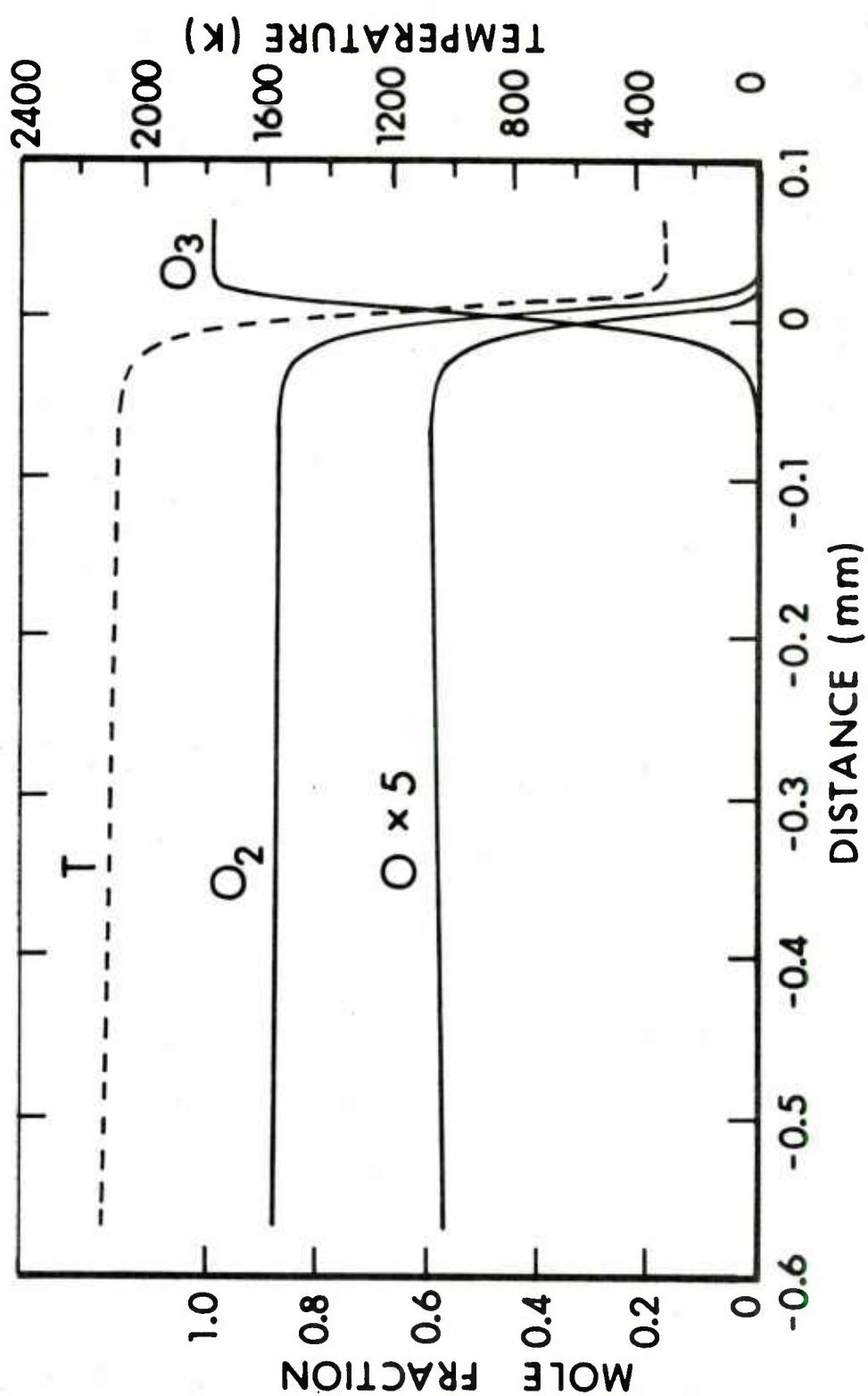


Figure 4. Temperature and Species Profiles for $10MF = 1.0$, $T_u = 300K$ and Total Pressure = 1 atmosphere.

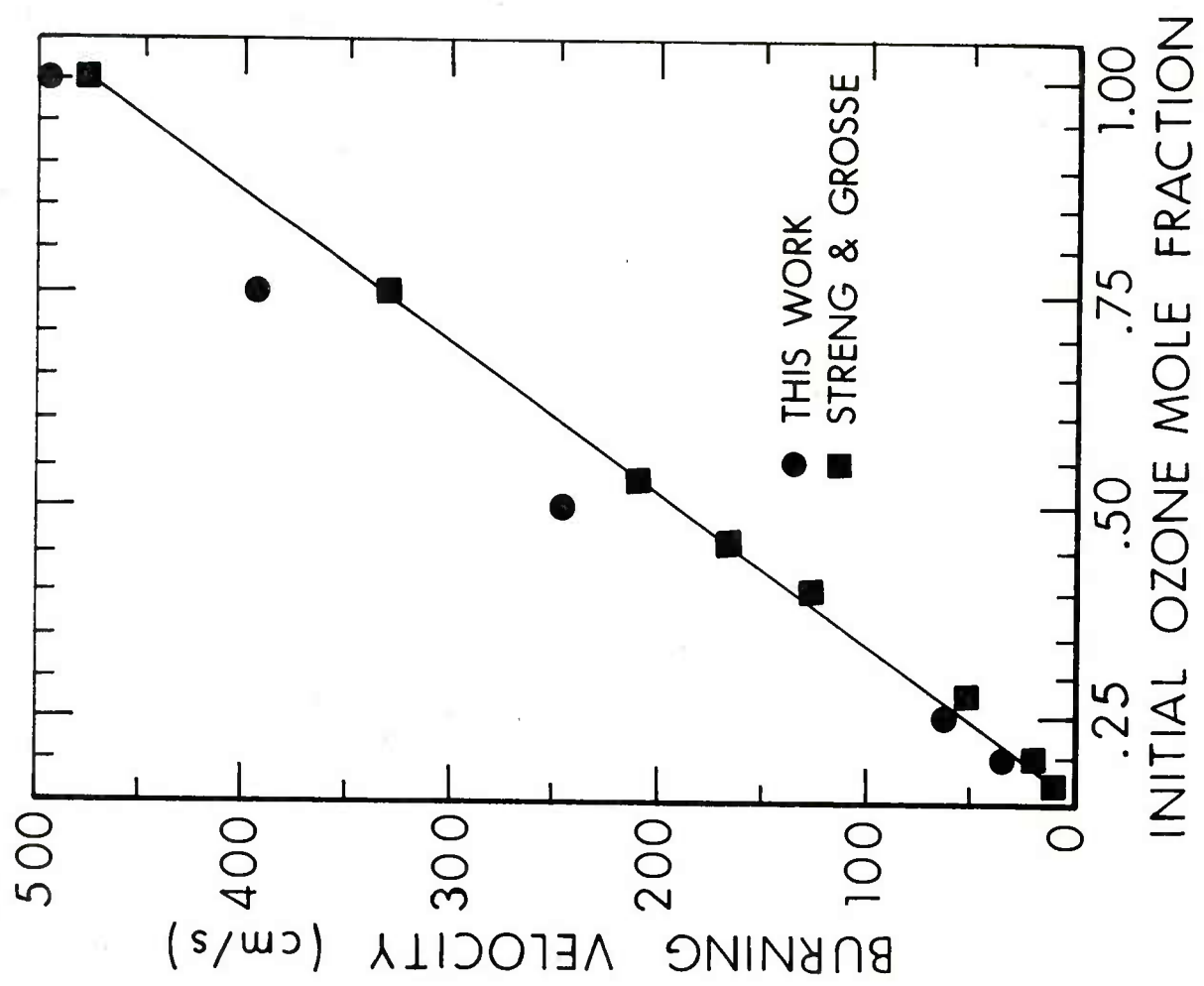


Figure 5. Burning Velocity vs. IOMF. Squares are the experimental points. Circles are computed from our model. The line is Streng and Grosse's expression for the burning velocity.

TABLE 5. COMPARISON OF OUR COMPUTED BURNING VELOCITIES
WITH THE MEASUREMENTS OF STRENG AND GROSSE

Initial Ozone Mole Fraction	Burning velocity (cm/s)		Ratio
	This work	Streng & Grosse*	
1.00	497	474	1.05
0.75	396	333	1.19
0.50	248	193	1.28
0.25	64	52	1.23
0.20	33	24	1.38

*Determined from equation (14).

breakpoints produced a maximum difference of 0.3% in the burning velocity computed using a given species (see equation (10)). By way of comparison the maximum species to species difference in the burning velocity was 0.4%. For IOMF = 1.0 we held the number of breakpoints fixed at 70 and subject to the condition NCC < KORD, varied both KORD and NCC over the range $3 \leq KORD \leq 8$ and $2 \leq NCC \leq 7$. The maximum change in the burning velocity computed from the atomic oxygen (O_2, O_3) profile was 2.6% (1%). A similar test for IOMF = 0.25 showed a maximum change of 1.9% (0.3%). We infer from the observed insensitivity that our standard conditions are sufficient to produce a numerically reliable solution. We also found that our computational efficiency could have been improved over our standard conditions by reducing both KORD and NCC by one or two.

Table 6 shows the percentage change in velocities of IOMF's of 0.25 and 1.00 for a given change in each of the kinetic and transport coefficients. (The kinetic coefficients have been altered in pairs so that the equilibrium constant remains the same). The factor of 1.2 is arbitrary; but we feel representative for the input coefficients except for k_3 (factor of two) and for λ_2 ($\leq 6\%$). Because of non-linear effects we do not expect these percentage changes to be quantitatively scaleable to other changes in the input coefficients; nonetheless, we shall use them to indicate trends in the relative importance of each coefficient.

Warnatz³ has recently and independently assembled a finite difference code that, like ours, requires species dependent input coefficients. He has found that the discrepancies in the model results of Dixon-Lewis,¹ Wilde,² Bledjian⁴ and Campbell⁵ are traceable to the different expressions for the input coefficients each used. In the light of this discussion,³ we confine our remarks to a comparison of our model results with those of Warnatz.

Table 7 shows the comparison of the burning velocity for five IOMF's. Warnatz' values were read from his Figure 6, curve labelled "M". The right hand column shows the ratio of Warnatz' computed burning velocity to ours. It is seen that the two model results agree within $\pm 12\%$ over the range $0.20 \leq IOMF \leq 1.00$. This agreement does not imply that the sets of input coefficients used in the respective models are equivalent.

Figure 6 plots the ratio of the values of Warnatz' input coefficients to our corresponding values over the temperature range $1000K \leq T \leq 2400K$. The striking features of this plot are the ratios for k_1 and k_2 . The value for the k_1 ratio falls from 0.92 at 1000K to 0.39 at 2400K while k_2 rises from 1.46 to 1.76 over the same temperature range. Since we had both used the same source¹⁷ for k_3 , its ratio is unity and is not shown in the Figure. (The reverse of all three reactions plays no significant part in the determination of the burning velocity and they are not further discussed.)

The ratios of the values of the transport coefficients are seen to be nearly independent of temperature (both Warnatz and we have used

TABLE 6. PERCENTAGE CHANGE IN THE COMPUTED BURNING VELOCITY
AT INITIAL OZONE MOLE FRACTIONS OF 0.25 AND 1.00 WHEN EACH
INPUT COEFFICIENT IS MULTIPLIED BY A FACTOR OF 1.2

Input Coefficient	% Change in Burning Velocity	
	0.25	1.00
k_1	8.6	4.6
k_2	0.8	4.4
k_3	0.0	0.0
λ_1	0.2	0.4
λ_2	11.8	3.6
λ_3	0.9	2.5
pD_{12}	2.7	1.9
pD_{13}	0.5	4.5
pD_{23}	-5.7	-3.6

TABLE 7. COMPARISON OF WARNATZ' COMPUTED
BURNING VELOCITIES WITH OURS

Initial Ozone Mole Fraction	Burning Velocity (cm/s)		Ratio
	Warnatz	This work	
1.00	445	497	0.90
0.75	350	396	0.88
0.50	225	248	0.91
0.25	65	64	1.02
0.20	37	33	1.12

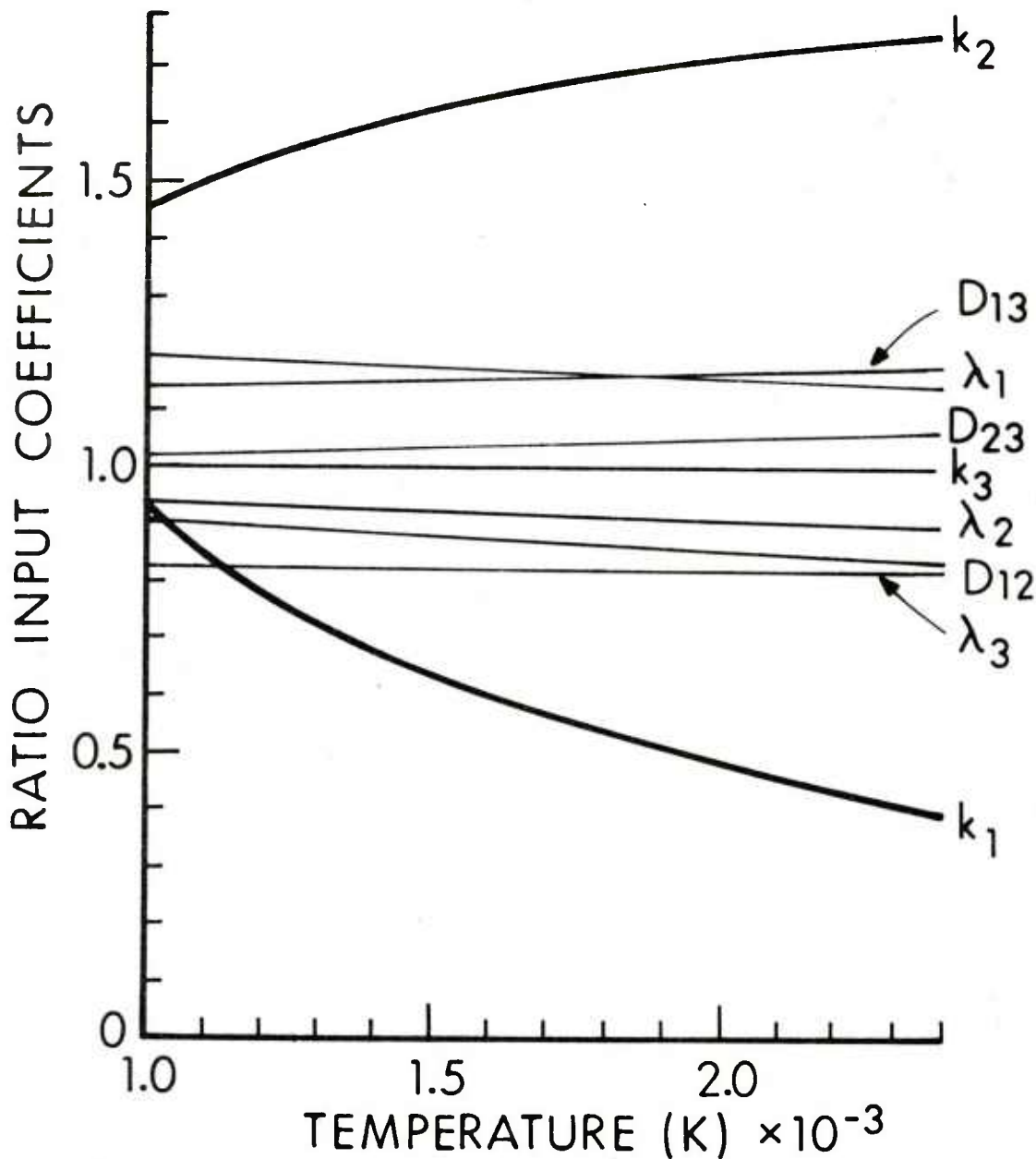


Figure 6. Ratio of the Values of Warnatz' and Our Input Coefficients; e.g., the ratio $k_1, \text{Warnatz}/k_1, \text{this paper}$ is given by the curve identified by k_1 .

similar functional forms) and the respective values of each ratio within $\pm 20\%$ of each other.* The important point is that the differences in transport coefficients are much less than those associated with the kinetic coefficients k_1 and k_2 .

If the kinetic coefficients for k_1 and k_2 differ by so much how can the burning velocities listed in Table 7 be in essential agreement? The answer is suggested by the sensitivities of the burning velocity to changes in k_1 and k_2 as listed in Table 6.

For the 1.00 IOMF the influence k_1 and k_2 upon the burning velocity are about equal; and, in going from one model to the other, the high temperature values of k_1 and k_2 change in opposite directions (see Figure 6). Thus in this case there is a tendency for the individual effects of k_1 and k_2 on the burning velocity to offset each other.

This tendency can be checked in the following manner. Using our model results for the burning velocity at an IOMF of 1.00 as a fiducial, we successively substitute into our model Warnatz' expressions for k_1 , then for k_2 , and finally for both k_1 and k_2 and compute the burning velocity in each case. As can be seen in Table 8 the burning velocity so computed, first goes down relative to the fiducial, then up and finally shows the mutually offsetting effects of these changes in k_1 and k_2 . As an added bonus the burning velocity of 459 cm/s obtained by substituting Warnatz' kinetic coefficients for k_1 and k_2 into our code (see Table 8) can be compared to Warnatz' own computed value of 445 cm/s to provide a measure of the collective effects of differing transport.

Table 6 shows that for the 0.25 IOMF case, the burning velocity's sensitivity to changes in kinetic coefficients is dominated by k_1 . Figure 6 shows that Warnatz' and our values for k_1 are much closer at the lower temperatures.

In comparing profiles there are sensible differences in some model results. For 1.00 IOMF, Figures 7 and 8 show a comparison of the atomic oxygen and temperature profiles, respectively. (Warnatz' values were read from his Figure 7). For ease in viewing, the curves have been arbitrarily displaced from each other along the distance axis in both figures. Figure 7 shows that within the burned region, behind the flame-front, i.e., -0.05 to -0.10mm, our computed value for the atomic oxygen mole fraction lies about a factor of two greater than Warnatz'. Figure 8 shows that over this same region our computed temperature lies about 350K below Warnatz'.

* We note that the L-J and Stockmayer parameters used by Warnatz are quite different than those used here. The fact that the transport values can be represented by different pairs of parameters has been discussed.^{8,27}

TABLE 8. SUCCESSIVE SUBSTITUTION OF WARNATZ' (W) KINETIC COEFFICIENTS FOR OURS (0) AT AN INITIAL OZONE FRACTION OF UNITY

k_1	k_2	Burning Velocity
0	0	497 cm/s
W	0	427
0	W	553
W	W	459

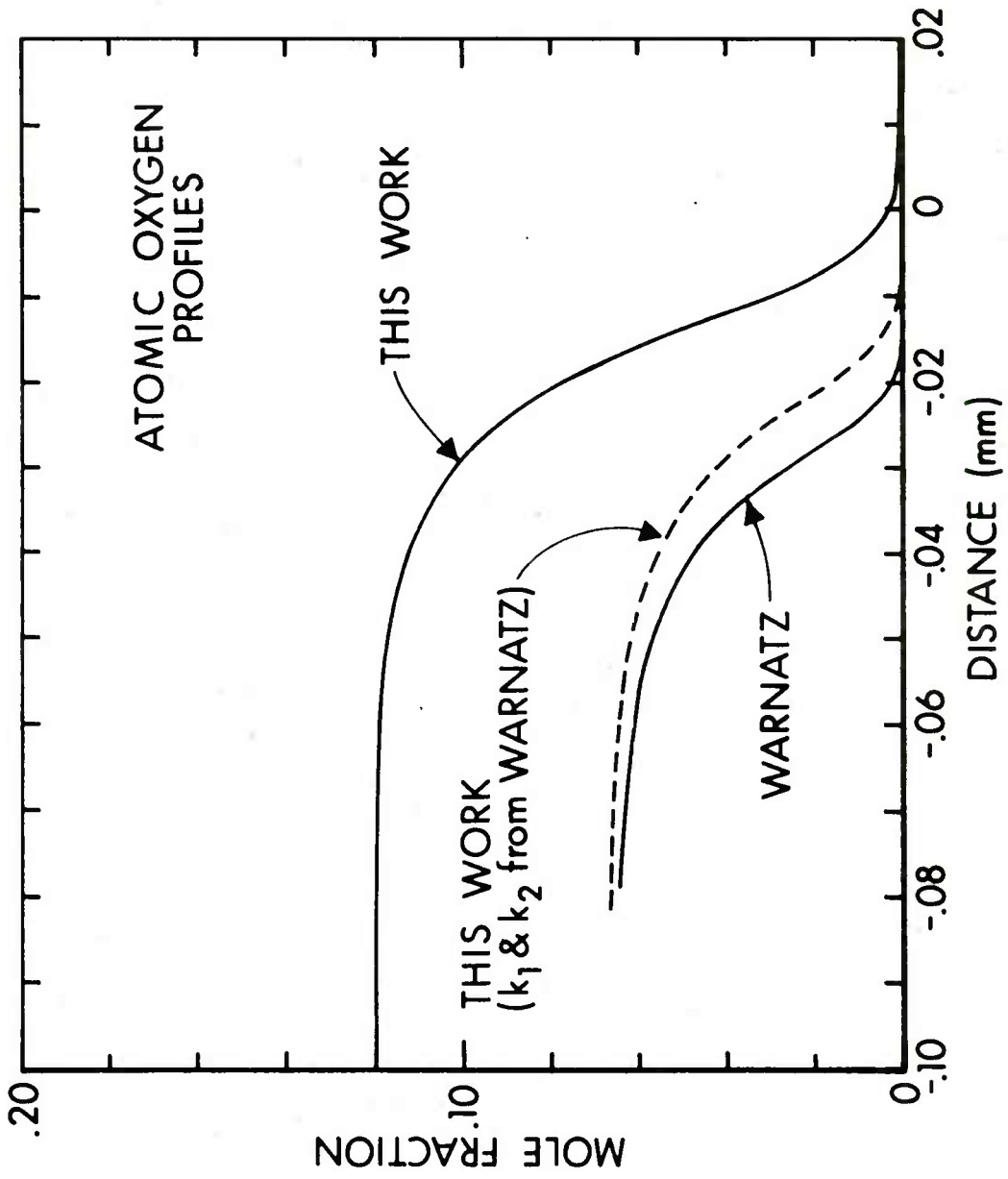


Figure 7. Our and Warnatz' Calculated Atomic Oxygen Profiles for $IOMF = 1.0$. (These curves are arbitrarily displaced for ease in viewing.) Dashed profile results for the substitution of Warnatz' expressions for k_1 and k_2 into our model.

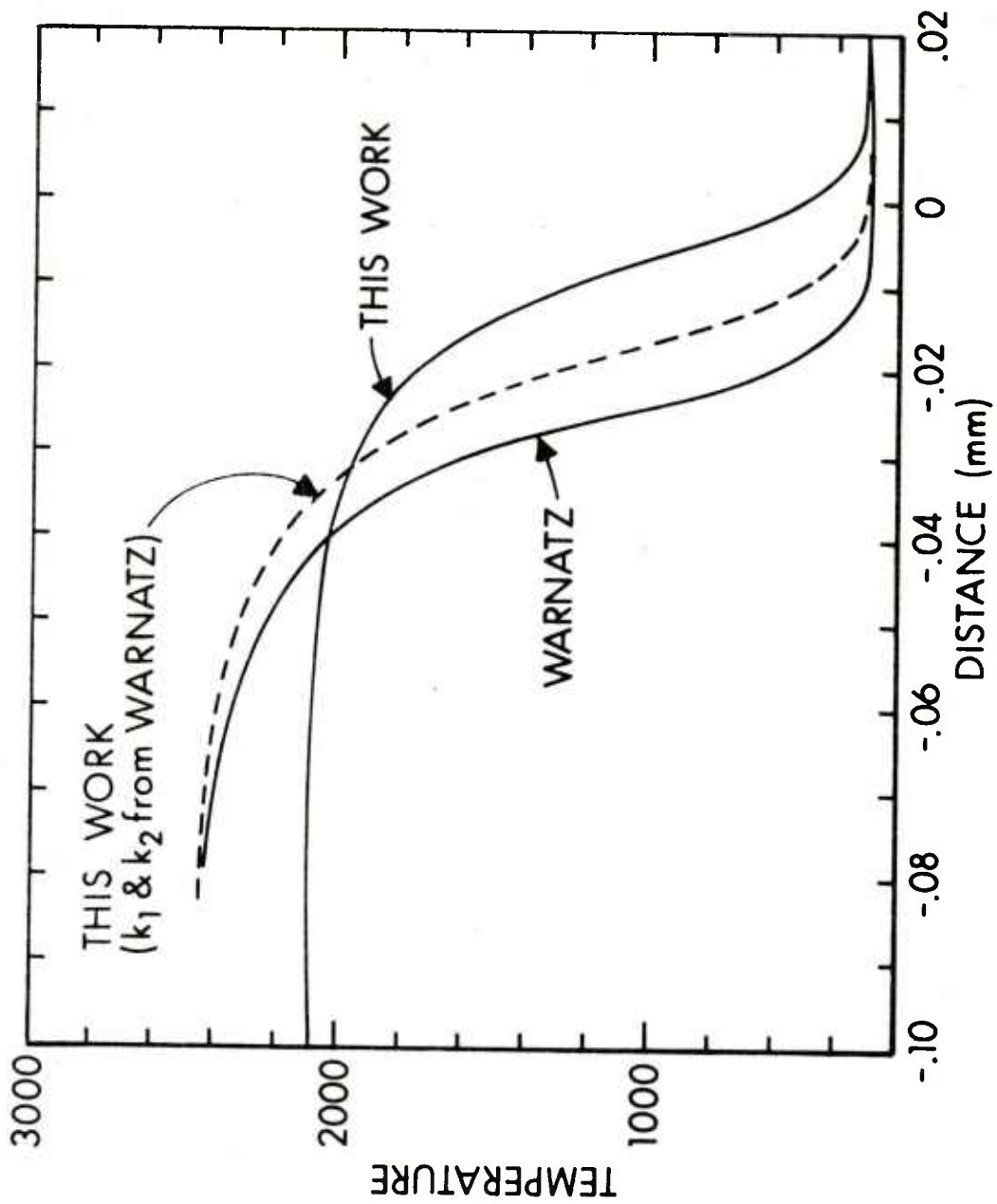


Figure 8. Our and Warnatz' Calculated Temperature Profiles for $IOMF = 1.0$. (These curves are arbitrarily displaced for ease in viewing.) Dashed profile results from the substitution of Warnatz' expressions for k_1 and k_2 into our model.

We now consider the causes of the profile differences. In the burned region, where the ozone concentration and the species and thermal gradients are small, the only reaction of importance is the atomic oxygen recombination reaction. (We find the effect of k_{-3} completely negligible which is equivalent to taking $k_{-3} = 0$ as was done by Warnatz.) As noted previously, both models employ the same expression¹⁷ for k_3 . Thus, the causes of these differences in the burned region must be sought in the flame-front. In this region, as we have seen, the main differences in the model input coefficients are the expressions for k_1 and k_2 . Substitution of Warnatz' expressions for k_1 and k_2 into our code yields the dashed line in both Figures 7 and 8. This substitution shows that the preponderance of the differences in these profiles is due to the different expressions for k_1 and k_2 . In other words these different expressions lead to different atomic oxygen superequilibrium concentrations and the relaxation to the final equilibrium state, via reaction (III), is so slow that these differences are effectively frozen.

The fact that both models employ the same expression for k_3 permits us to check on the models' mutual consistency in the burned region. To wit, the atomic oxygen difference between model results as seen in Figure 7 is sufficient to account for the temperature difference between the models' results as seen in Figure 8.

For 0.20 IOMF, the values of the controlling input coefficients for the two models are similar. We expect and find similar species and temperature profiles (not shown).

We have found that the area of a greatest discrepancy in the input values used for these two models lies in the expressions used for the two rate coefficients, k_1 and k_2 . We have recently critically evaluated the available high temperature experimental data for the ozone decomposition reaction and the expression used herein is consistent with all the direct experimental data known to the authors.¹⁸ (In order to use the various experimental data to obtain the ozone decomposition expression we have assumed that the relative third body efficiencies are independent of temperature).

The expression used for k_2 is another story. Warnatz has developed and used his own expression⁴⁰ and we have employed Hampson's.²¹ To use them in our codes we have both assumed that the respective expressions are valid beyond the upper limit of applicability of each, i.e., 1000K.

In order to distinguish which expression for k_2 , if either, is correct, measurements and/or *ab initio* calculations of the rate coefficient for reaction (II) are required at high temperatures, say in the range 1500-2000K. Alternately, the computed differences in the values for atomic oxygen and the temperature in the burned region at an IOMF

⁴⁰J. Warnatz, "Berechnung der Flammengeschwindigkeit und der Struktur von laminaren flachen Flammen", *Habilitationsschrift, Darmstadt, 1977.*

of 1.00 appear to be large enough that profile measurements above a flame may be sufficient to distinguish between the two expressions.

VI. SUMMARY

We have shown that this model and its input parameters (see Tables 1, 2, and 3) predict burning velocities that are in reasonable agreement with the measurements of Streng and Grosse³⁹ and with the computations of Warnatz.³ We have also demonstrated that agreement with burning velocities, even over a wide range of initial ozone mole fractions, is a necessary but not sufficient condition to ensure that the input coefficients are realistic. We have shown that profile measurements are vital to test the model's input coefficients and so validate the model. Finally, by a comparison of computed profiles we have indicated the need to measure or to calculate high temperature values for k_2 .

REFERENCES

1. F. Cramarossa and G. Dixon-Lewis, "Ozone Decomposition in Relation to the Problem of the Existence of Steady-State Flames", *Combustion and Flame* 16, 243-251 (1971).
2. Kenneth A. Wilde, "Boundary-Value Solutions of the One-Dimensional Laminar Flame Propagation Equations", *Combustion and Flame* 18, 43-52, (1972).
3. J. Warnatz, "Calculation of the Structure of Laminar Flat Flames I: Flame Velocity of Freely Propagating Ozone Decomposition Flames", *Ber. Bunsenges Phys. Chem.* 82, 193-200 (1978).
4. Leon Bledjian, "Computation of Time-Dependent Laminar Flame Structure", *Combustion and Flame* 20, 5-17, (1973).
5. Edwin S. Campbell, "A Theoretical Analysis of Chemical and Physical Processes in an Ozone Flame", *Chem. Engineering Sci.* 20, 311-329, (1965).
6. Stephen B. Margolis, "Time-Dependent Solution of a Premixed Laminar Flame", *J. of Computational Phys.* 27, 410-427, (1978).
7. J. O. Hirschfelder, C. F. Curtis and Dorothy E. Campbell, "The Theory of Flame Propagation. IV", *J. Phys. Chem.* 57, 403-414, (1953).
8. J. O. Hirschfelder, C. F. Curtis and R. B. Bird, Molecular Theory of Gases and Liquids, 2nd Printing, Corrected, with notes, John Wiley and Sons, NY, (1964).
9. R. B. Bird, W. S. Stewart and E. N. Lightfoot, Transport Phenomena, John Wiley and Sons, NY, (1960).
10. F. A. Williams, Combustion Theory, Addison-Wesley, Reading, MA, (1965).
11. R. M. Fristrom and A. A. Westenberg, Flame Structure, McGraw-Hill, NY, (1965) p. 319.
12. B. K. Madsen and R. F. Sincovec, "PDECOL: General Collocation Software for Partial Differential Equations", Preprint UCRL-78263 (Rev 1) Lawrence Livermore Laboratory, (1977).
13. C. de Boor, "Package for Calculating With B-Splines", *Siam. J. Numer. Anal.* 14, 441-472, (1977).
14. T. P. Coffee and J. M. Heimerl, "A Method for Computing the Flame Speed for a Laminar, Premixed, One Dimensional Flame", BRL Technical Report, ARBRL-TR-02212, Jan 80. (AD#A082803)

REFERENCES (Cont'd)

15. D. B. Spalding and P. L. Stephenson, "Laminar Flame Propagation in Hydrogen and Bromine Mixtures", Proc. Roy. Soc. London A324, 315-337, 1971. (See also), D. B. Spalding, P. L. Stephenson and R. G. Taylor, "A Calculation Procedure for the Prediction of Laminar Flame Speeds", Combustion and Flame, 17, 55-64, 1971.
16. D. L. Baulch, D. D. Drysdale, J. Duxbury and S. J. Grant, Evaluated Kinetic Data for High Temperature Reactions, Vol 3, Homogeneous gas phase reactions of the O₂/O₃ system, the CO/O₂/H₂ system and of sulphur containing species. Butterworths, Boston, (1976).
17. Harold S. Johnston, "Gas Phase Reaction Kinetics of Neutral Oxygen Species", NSRDS-NBS-20, September 1968.
18. J. M. Heimerl and T. P. Coffee, "The Unimolecular Ozone Decomposition Reaction", Combustion and Flame, 35, 117-123, 1979. For a complete listing of all direct measurements, see BRL Technical Report ARBRL-TR-02185, Aug 79. (AD#A076966)
19. J. V. Michael, "Thermal Decompositon of Ozone", J. Chem. Phys. 54, 4455-4459, (1971).
20. R. E. Center and R. T. V. Kung, "Shock Tube Study of the Thermal Decomposition of O₃ From 1000 to 3000°K", J. Chem. Phys. 62, 801-807, (1975).
21. R. F. Hampson, (ed), "Survey of Photochemical and Rate Data for Twenty-Eight Reactions of Interest in Atmospheric Chemistry", J. Phys. Chem. Ref. Data 2, 267-312, (1973).
22. D. R. Stull and H. Prophet, JANAF Thermochemical Tables, 2nd Edition, NSRDS-NBS-37, June 1971.
23. S. Gordon and B. J. McBride, "Computer Program for Calculation of Complex Chemical Equilibrium Compositions, Rocket Performance, Incident and Reflected Shocks, and Chapman-Jouguet Detonations", NASA-SP-273, (1971), (1976 program version).
24. A. Dalgarno and F. J. Smith, "The Thermal Conductivity and Viscosity of Atomic Oxygen", Planet Spac. Sci. 9, 1-2, (1962).
25. H. J. M. Hanley and J. F. Ely, "The Viscosity and Thermal Conductivity Coefficients of Dilute Nitrogen and Oxygen", J. Phys. Chem. Ref. Data, 2, 735-755, (1973).
26. T. R. Marrero and E. A. Mason, "Gaseous Diffusion Coefficients", J. Phys. Chem. Ref. Data, 1, 3-118, (1972).

REFERENCES (Cont'd)

27. R. C. Reid and T. K. Sherwood, The Properties of Gases and Liquids, 2nd Edition, McGraw-Hill, NY, (1966).
28. J. O. Hirschfelder, C. F. Curtis and R. B. Bird, op. cit., p. 562.
29. R. A. Svehla, "Estimated Viscosities and Thermal Conductivities of Gases at High Temperatures", NASA Tech. Report R-132, Lewis Res. Ct., Cleveland, Ohio, (1962).
30. V. J. Tretter, An Experimental Determination of the Viscosity of Gaseous Ozone, M. S. thesis, U. of Idaho, (1966), unpublished.
31. J. O. Hirschfelder, C. F. Curtis and R. B. Bird, op. cit., p. 530.
32. J. O. Hirschfelder, C. F. Curtis and R. B. Bird, op. cit., p. 600.
33. J. O. Hirschfelder, C. F. Curtis and R. B. Bird, op. cit., p. 950.
34. A. L. McCellan, Tables of Experimental Dipole Moments, W. H. Freeman and Co., San Francisco, (1963).
35. J. H. Hildebrand, Mole. Phys. 35, 519-523, (1978).
36. V. V. Yastrebov, "The Physical Chemistry of Concentrated Ozone, VIII. Thermal Propagation of Flame in Gaseous Ozone Mixtures", Russian J. of Phys. Chem., 34, 21-23, (1960).
37. J. L. Houzclot and J. Villermieux, "Measurement of the Molecular Diffusivity of Ozone Oxygen", C. R. Acad. Sci. Ser. C. 1971, 273, 258-60. As quoted by Chem. Abstracts 74, 252, (1971).
38. Y. S. Touloukian, P. E. Liley and S. C. Saxena, Thermophysical Properties of Matter, Vol. 3, Thermal Conductivity, (Nonmetallic Liquids and Gases), IFI/Plenum, NY-Washington, (1970), p 45a.
39. A. G. Streng and A. V. Grosse, "The Ozone to Oxygen Flame", Sixth Symposium (International) on Combustion, Reinhold Publishing Company, (1957), pp 264-273.
40. J. Warnatz, "Berechnung der Flammengeschwindigkeit und der Struktur von laminaren flachen Flammen", Habilitationsschrift, Darmstadt, 1977.

GLOSSARY

C_p	= Heat capacity at constant pressure, cal-mole $^{-1}$ -K $^{-1}$
c_p	= $\sum c_{pi} Y_i$, the specific heat of the mixture, cal-gm $^{-1}$ -K $^{-1}$
c_{pi}	= specific heat of ith species, cal-gm $^{-1}$ -K $^{-1}$
D_{kj}	= binary diffusion coefficient for species k and j, cm 2 -s $^{-1}$
H_T^o	= enthalphy, cal-mole $^{-1}$
h_i	= specific enthalpy, cal-gm $^{-1}$
k	= Boltzmann's constant, = 1.3806 erg - K $^{-1}$
k_i	= rate coefficient for the ith reaction, in centimeter-mole-seconds units
N	= number of species
M_i	= molecular weight of ith species, gm-mole $^{-1}$
m_o	= mass flux, gm-cm $^{-2}$ -s $^{-1}$
p	= total pressure, atmosphere
R	= Gas constant, = 1.9872 cal-mole $^{-1}$ K $^{-1}$, = 82.05 cm 3 -atmos-mole $^{-1}$ -K $^{-1}$
R_i	= Rate of production of ith species by chemical reactions, mole-cm $^{-3}$ -s $^{-1}$
S_u	= burning velocity, cm-s $^{-1}$
T	= temperature, K
T_i^*	= $T(\epsilon_i/k)^{-1}$
T_u	= temperature of unburned mixture, K
t	= temporal coordinate, s
u	= fluid velocity, cm-s $^{-1}$
v_i	= diffusion velocity of ith species, cm-s $^{-1}$
x	= spatial coordinate, cm
X_i	= mole fraction of ith species

Y_i = mass fraction of ith species

Y_{iu} = mass fraction of ith species in the unburned mixture

ϵ_i/k = L-J or Stockmayer parameter, K

η_i = viscosity of ith species, $\text{gm-s}^{-1}\text{-cm}^{-1}$

λ = mixture conductivity, $\text{cal-cm}^{-1}\text{-s}^{-1}\text{-K}^{-1}$

λ_i = conductivity of ith species, $\text{cal-cm}^{-1}\text{-s}^{-1}\text{-K}^{-1}$

σ_i = L-J or Stockmayer parameter, $10^{-8}\text{cm} (= \text{\AA})$

ρ = fluid density, gm-cm^{-3}

ψ = Lagrangian coordinate (see equation 6), gm-cm^{-2}

$\Omega^{1,2}, \Omega^{2,2}$ = collision intergrals (tabulated in reference 8)

DISTRIBUTION LIST

<u>No. of Copies</u>	<u>Organization</u>	<u>No. of Copies</u>	<u>Organization</u>
12	Commander Defense Technical Info Center ATTN: DDC-DDA Cameron Station Alexandria, VA 22314	1	Commander US Army Armament Materiel Readiness Command ATTN: DRSAR-LEP-L, Tech Lib Rock Island, IL 61299
1	Director Defense Advanced Research Projects Agency ATTN: LTC C. Buck 1400 Wilson Boulevard Arlington, VA 22209	1	Director US Army ARRADCOM Benet Weapons Laboratory ATTN: DRDAR-LCB-TL Watervliet, NY 12189
2	Director Institute for Defense Analyses ATTN: H. Wolfhard R.T. Oliver 400 Army-Navy Drive Arlington, VA 22202	1	Commander US Army Watervliet Arsenal ATTN: Code SARWV-RD, R. Thierry Watervliet, NY 12189
1	Commander US Army Materiel Development & Readiness Command ATTN: DRCDMD-ST 5001 Eisenhower Avenue Alexandria, VA 22333	1	Commander US Army Aviation Research & Development Command ATTN: DRSAV-E P.O. Box 209 St. Louis, MO 63166
2	Commander US Army Armament Research & Development Command ATTN: DRDAR-TSS Dover, NJ 07801	1	Director US Army Air Mobility Research & Development Laboratory Ames Research Center Moffett Field, CA 94035
5	Commander US Army Armament Research & Development Command ATTN: DRDAR-LCA, J. Lannon DRDAR-LC, T. Vladimiroff DRDAR-LCE, F. Owens DRDAR-SCA, L. Stiefel DRDAR-LC, D. Downs Dover, NJ 07801	1	Commander US Army Communications Research & Development Command ATTN: DRDCO-PPA-SA Ft. Monmouth, NJ 07703
			Commander US Army Electronics Research & Development Command Technical Support Activity ATTN: DELSD-L Fort Monmouth, NJ 07703

DISTRIBUTION LIST

<u>No. of Copies</u>	<u>Organization</u>	<u>No. of Copies</u>	<u>Organization</u>
2	Princeton University Forrestal Campus ATTN: I. Glassman Tech Lib P.O. Box 710 Princeton, NJ 08540	1	University of Illinois Dept of Aeronautical Engineering ATTN: H. Krier Transportation Bldg, Rm 105 Urbana, IL 61801
2	Purdue University School of Mechanical Engineering ATTN: J. Osborn S.N.B. Murthy TSPC Chaffee Hall West Lafayette, IN 47906	1	University of Minnesota Dept of Mechanical Engineering ATTN: E. Fletcher Minneapolis, MN 55455
1	Rutgers State University Dept of Mechanical and Aerospace Engineering ATTN: S. Temkin University Heights Campus New Brunswick, NJ 08903	1	University of Southern California Dept of Chemistry ATTN: S. Benson Los Angeles, CA 90007
4	SRI International ATTN: Tech Lib D. Crosley J. Barker D. Golden 333 Ravenswood Avenue Menlo Park, CA 94025	1	University of Texas Dept of Chemistry ATTN: W. Gardiner H. Schaefer Austin, TX 78712
2	University of Utah Dept of Chemical Engineering ATTN: A. Baer G. Flandro Salt Lake City, UT 84112		
1	Stevens Institute of Technology Davidson Library ATTN: R. McAlevy, III Hoboken, NJ 07030		<u>Aberdeen Proving Ground</u>
1	University of California, San Diego Ames Department ATTN: F. Williams P.O. Box 109 La Jolla, CA 92037		Dir, USAMSAA ATTN: DRXSY-D DRXSY-MP, H. Cohen
		Cdr, USATECOM ATTN: DRSTE-TO-F	
		Dir, Wpns Sys Concepts Team Bldg E3516, EA ATTN: DRDAR-ACW	

USER EVALUATION OF REPORT

Please take a few minutes to answer the questions below; tear out this sheet and return it to Director, US Army Ballistic Research Laboratory, ARRADCOM, ATTN: DRDAR-TSB, Aberdeen Proving Ground, Maryland 21005. Your comments will provide us with information for improving future reports.

1. BRL Report Number _____

2. Does this report satisfy a need? (Comment on purpose, related project, or other area of interest for which report will be used.)

3. How, specifically, is the report being used? (Information source, design data or procedure, management procedure, source of ideas, etc.)

4. Has the information in this report led to any quantitative savings as far as man-hours/contract dollars saved, operating costs avoided, efficiencies achieved, etc.? If so, please elaborate.

5. General Comments (Indicate what you think should be changed to make this report and future reports of this type more responsive to your needs, more usable, improve readability, etc.)

6. If you would like to be contacted by the personnel who prepared this report to raise specific questions or discuss the topic, please fill in the following information.

Name: _____

Telephone Number: _____

Organization Address: _____